Electromagnetic dissociation of ^{59}Co and ^{197}Au targets by relativistic ^{139}La projectiles

John C. Hill, F. K. Wohn, J. A. Winger, M. Khayat, and K. Leininger

Ames Laboratory and Iowa State University, Ames, Iowa 50011

A. R. Smith

Lawrence Berkeley Laboratory, Berkeley, California 94720

The electromagnetic dissociation of ^{59}Co and ^{197}Au target nuclei by 1.26 GeV/nucleon ^{139}La projectiles was inferred from measurement of cross sections for the one-neutron removal reaction. The corresponding electromagnetic dissociation cross sections are large, reaching 0.28 ± 0.04 and 1.97 ± 0.13 barns for the ^{59}Co(^{139}La,X)^{58}Co and ^{197}Au(^{139}La,X)^{196}Au reactions, respectively. The experimental cross sections in excess of the estimated nuclear contributions are generally well described by use of the Weizsäcker-Williams method for calculating the electromagnetic dissociation contributions, but they appear to increase more slowly as the projectile charge is increased, consistent with a trend observed earlier for lower-Z projectiles.

I. INTRODUCTION

Dissociation of relativistic heavy ions (RHI) by the Coulomb fields of target nuclei, called electromagnetic dissociation (ED), was first reported by Heckman and Lindstrom.[1] Evidence was seen for ED in both the single-neutron and the single-proton channels for 2.1 GeV/nucleon ^{12}C and ^{16}O and 1.05 GeV/nucleon ^{12}C projectiles. Olson et al.[2] observed ED in the fragmentation of 1.7 GeV/nucleon ^{18}O projectiles by targets ranging from Be to U. ED cross sections were measured for ^{17}O, ^{16}O, and ^{17}N projectile-like fragments which correspond to one-neutron, two-neutron, and one-proton removal processes, respectively. The largest ED cross section was 140.8 mb for U(^{18}O,^{17}O)X.

ED was first reported for target fragmentation by Mercier et al.[3] In those experiments ^{59}Co, ^{89}Y, and ^{197}Au targets were bombarded with RHI ranging from 2.1 GeV/nucleon ^{12}C to 1.7 GeV/nucleon ^{56}Fe. The one-neutron removal ED cross sections became quite large[4] as the projectile Z increased, reaching 601 mb for the ^{197}Au(^{56}Fe,X)^{196}Au reaction.

ED can be pictured as a purely electromagnetic process which occurs when RHI pass near a high-Z target nucleus but outside the range of the nuclear force. A virtual photon from the Coulomb field is absorbed by either the target or the projectile, resulting in its excitation, usually to a giant multipole resonance, which subsequently deexcites by particle emission. Competing with ED is the process of nuclear fragmentation which can also result in the loss of one neutron. ED, which is an electromagnetic process, can occur over a large range of impact parameters, but nuclear fragmentation is limited by the short range of the nuclear force.

ED cross sections have been calculated[1-4] from a virtual photon spectrum obtained using the Weizsäcker-Williams procedure.[5] Although agreement is satisfactory, discrepancies for the largest σ_{ED} values have been observed.[4] Recent calculations by Baur and Bertulani[6] and

Mercier et al.[4] indicate that, for the projectile energies of 100 GeV/nucleon expected for the planned RHIC heavy-ion collider, the ^{238}U on ^{238}U (Ref. 6) and ^{197}Au on ^{197}Au (Ref. 4) σ_{ED} values could reach 40 and 24 barns, respectively, for fixed targets.

Since it is not possible to experimentally check the above predictions at the present time, we have endeavored to determine the Z dependence of the ED process by extending our previous results to higher-Z projectiles at Bevalac energies. We report in this paper detailed results of measurements using 1.26 GeV/nucleon^{139}La projectiles on ^{59}Co and ^{197}Au targets. These results have been reported in preliminary form orally[7] and in a recent letter.[8]

II. CALCULATION OF ELECTROMAGNETIC DISSOCIATION CROSS SECTIONS

In order to calculate cross sections for the ED process we form the product of the virtual photon spectrum $N_\gamma(E_\gamma)$ with that of the appropriate photonuclear cross section $\sigma_\gamma(E_\gamma)$. This process is indicated for the ^{197}Au(^{139}La,X)^{196}Au reaction in Fig. 1. In order to get the ED cross section σ_{ED} we integrate the above product:

$$\sigma_{ED} = \int_0^\infty N_\gamma(E_\gamma)\sigma_\gamma(E_\gamma)dE_\gamma .$$

The $\sigma_\gamma(E_\gamma)$ used in our calculations for each of the targets is discussed in Sec. V A.

Two methods have been used for calculating $N_\gamma(E_\gamma)$; the Weizsäcker-Williams (WW) method for virtual photons[5] which assumes a point charge, and the method of Jäckle and Pilkuhn[9] (JP) which assumes a Yukawa charge distribution. In the case of projectile fragmentation, the JP method is quite insensitive to the charge distribution of the target. In this case, the results using a Gaussian charge distribution and those using a point charge were the same within the error of the measured photonuclear cross sections. (See, for example, Fig. 3 in
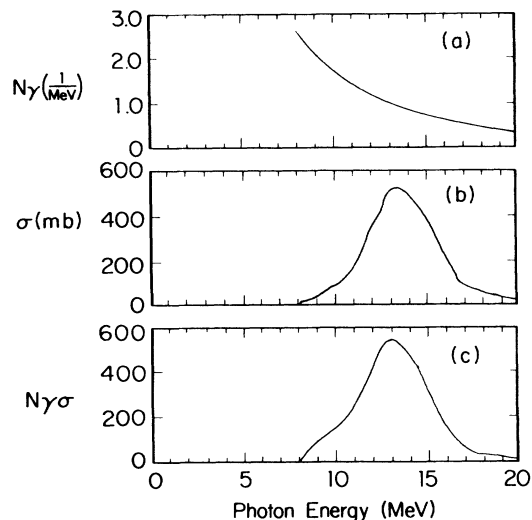
FIG. 1. Components necessary for calculation of the electromagnetic dissociation cross section σ_{ED}. (a) shows the virtual-photon spectrum N_γ for 1.26 GeV/nucleon ^{139}La projectiles calculated using the Weizsäcker-Williams method. (b) shows the ^{197}Au(γ,n)^{196}Au photonuclear cross section taken from Ref. 28. (c) shows the product of (a) and (b) that is integrated to obtain σ_{ED}. To obtain the correct σ_{ED} the above integral must be multiplied by 0.93 as discussed in Sec. V A.

Ref. 2.) Unfortunately, the difference in the JP and WW calculations for a point charge differ by about 30%. This problem associated with these two methods has been discussed in some detail.[2,4]

Many of the WW calculations of virtual photon spectra used in the analysis of the ED effect have ignored contributions due to multipoles other than $E1$. Goldberg[10] has determined the virtual photon spectrum for RHI on stationary targets for all multipoles. Contributions to ED from $M1$ transitions are expected to be negligible,[10] but the contribution from $E2$ can be significant, since for $\gamma = 3\{\gamma = [1-(v^2/c^2)]^{-1/2}\}$ the $E2$ virtual photon spectrum exceeds that for $E1$ by about a factor of 3. Goldberg found that for $\gamma = 3$ the ratio of $E2$ to $E1$ strengths is 0.09 for ^{238}U projectiles on a ^{238}U target. Bertulani[11] has calculated the ratio $\sigma_{ED}(E2)/\sigma_{ED}(E1)$ for the cases studied[4] by us. In all cases the ratio is approximately 0.2 which is not negligible, but in our results the error only comes in to the extent that the $E2/E1$ mixture is different for real and virtual photons.

III. EXPERIMENTAL METHOD

A. Irradiation and counting procedures

The experimental methods employed are similar to those used by us in earlier experiments and discussed in detail in Ref. 4, but are briefly presented here. The bombardments were carried out in the external beam at the Lawrence Berkeley Laboratory (LBL) Bevalac accelerator using 1.26 GeV/nucleon ^{139}La projectiles. The tar-

gets consisted of foils of the monoisotopic elements Co and Au. Each target foil was placed between an Al foil (0.038-mm thick) on the upstream side and a Mylar foil (0.13-mm thick) on the downstream side. The Al foils were used to obtain a transverse beam intensity profile by counting ^{24}Na, and the Mylar served as a rigid backing for the target. Three different thicknesses of each target foil were bombarded simultaneously in order to obtain corrections for secondary reactions which are significant for one-neutron removal processes.

In order to obtain a good beam calibration, a target string was irradiated for 20 min and the beam intensity was obtained by measuring the yield of ^{11}C in the ^{12}C(^{139}La,X)^{11}C reaction in a 0.159 cm polystyrene target using a well-calibrated NaI(T1) γ spectrometer. The cross section for the ^{12}C(^{139}La,X)^{11}C reaction was accurately measured in a separate experiment.[12] This thin polystyrene target was positioned first in the target string to minimize the production of ^{11}C from secondary products produced in the other targets. Next in the string came three metal targets of the same thicknesses as those used for the main run. The last target in the string was a thick 5.08 cm polystyrene block in which the long-lived (53.3 d) ^{7}Be activity could be accurately measured and compared to ^{11}C activity in the thin upstream polystyrene target. This procedure enabled us to transfer the ^{11}C beam calibration function to thick-target ^{7}Be activity, thus providing a suitable absolute beam monitor for the much longer main experimental runs. The last device in the experimental array was an ion chamber which was used to compare total beam on target during the short and long runs, and measure fluctuations in beam intensity that must be used to make corrections to the yield calculations.

Next, two long runs lasting 17 and 4 h for the ^{197}Au and ^{59}Co targets, respectively, were carried out using new target strings, but with identical target parameters. In this run the metal targets were positioned first in the string in order to minimize secondary reactions in the metal. The metal targets increased in thickness as one went downstream and were each separated by 25 cm to minimize secondary reactions produced by cross talk between targets. The different thicknesses were used to correct for secondary reactions within the target and were 47, 113, and 227 mg/cm^2 for ^{59}Co and 49, 87, and 233 mg/cm^2 for ^{197}Au.

After irradiation all metal targets were shipped by air to the Ames Laboratory at Iowa State University for counting of the appropriate residual γ-ray activities using a low-energy photon spectrometer (LEPS) and two Ge detectors calibrated for absolute efficiency using NBS standard sources. The counting continued for periods as long as one year with dead-time corrections of less than 0.2%. The decays of isotopes were followed in most cases for several half-lives and corrections for interfering activities were made. The decay curves were fit using known half-lives and the appropriate yields were calculated using data from the thinnest target to minimize the corrections due to secondary particles. Information on beam intensity and target geometry was then included to obtain cross sections for the reactions of interest.

B. Corrections and error analysis

All targets were mounted on a 0.13 mm Mylar backing. It was determined by counting several of the Mylar backings after irradiation that loss of reaction products out of the target due to recoil was negligible due to the fact that relatively thick targets were used. Systematic errors can arise due to the finite spread and nonuniformity of the beam intensity. The finite spread of the beam on the target was determined by counting the ^{24}Na activity in a 0.038 mm Al foil on the upstream side of each of the targets. After irradiation the Al foil was cut into a 1.3-cm diameter central circle and three concentric rings of successively 2.5, 3.8, and 5.1 cm in outer diameter and counted. The information obtained was used to make source geometry corrections for the counting of γ rays using Ge detectors. It was also necessary to make corrections for geometry-dependent coincidence summing. In order to make the above correction, total efficiencies of our detectors were determined using ^{57}Co, ^{203}Hg, ^{113}Sn, ^{85}Sr, ^{54}Mn, ^{65}Zn, and ^{88}Y sources.

Generally the most significant corrections were those for production of a nuclide due to secondary reactions in the target. For deep spallation products, these corrections were negligible, but for the one-neutron removal products (mass close to that of target nucleus) the typical secondary reaction rate was several percent of the primary reaction rate. Secondary production from target-like fragments due to cross talk between the targets was negligible due to the fact that targets were separated by a distance of 25 cm. In each case, three targets of successively larger thicknesses were simultaneously irradiated. For corrections due to secondary particles absorbed by the same target in which they were produced, we assumed $N(t)=at+bt^2$ where a and b are constants, and $N(t)$ gives the amount of activity produced as a function of target thickness t. Parameter b would be 0 if secondary processes were negligible. $N(t)$ was measured for each of the three targets. For a given thickness t the secondary-to-primary ratio is bt/a.

C. Determination of cross sections

The experimental cross sections were determined from the expression

$$\sigma(\text{cm}^2) = \frac{N(\text{atoms/sec})M(\text{g/mole})}{f(\text{proj/sec})\rho(\text{g/cm}^2)N_a(\text{atoms/mole})} .$$

The target density ρ was determined by weighting our 5.1 cm by 5.1 cm targets on an analytical balance, and the total beam flux f was determined from the ^{11}C and ^{7}Be measurements. N, the disintegration rate at saturation, was determined from the γ-ray count rate by

$$N\left[\frac{\text{atoms}}{\text{sec}}\right] = \frac{n\left[\frac{\text{counts}}{\text{sec}}\right]}{\lambda\varepsilon bGB} .$$

n refers to counts per second at saturation and ε, b, G, and B represent absolute detector efficiency, γ-ray branching ratio, γ-ray absorption in the target, and correction for finite width of the irradiated spot, respectively.

IV. CROSS-SECTION RESULTS

A. One-neutron removal cross sections

In what follows the term one-neutron removal refers to processes in which one neutron but no protons are removed from the target nucleus. The independent yield of ^{58}Co ($T_{1/2}=70.82$ d) was determined by following the decay of the 811-keV γ ray which is 99.5% abundant.[13] Both ^{58}Ni and ^{58}Fe are stable. The independent yield of ^{196}Au ($T_{1/2}=6.183$ d) was determined by measuring the decay of the 333- and 355-keV γ rays which are 22.9% and 86.9% abundant,[14] respectively. Both ^{196}Hg and ^{196}Pt are stable. The experimental cross sections for the one-neutron removal reactions are given in Table I.

B. Factorization and limiting fragmentation

In order to estimate the nuclear contribution to the total cross section, we make use of the concept of factorization[15] of the nuclear cross section. This assumes $\sigma^F_{TP}=\gamma^F_T\gamma^T_P$, where F, T, and P indicate dependencies on target fragment, target, and projectile, respectively. This notation is similar to that of Heckman and Lindstrom[1] but with the roles of P and T reversed. Factorization implies that the yield of a particular fragment from the target due to nuclear interactions will be independent of the beam except through the geometric factor γ^T_P. Thus, for example, the ratio

$$\sigma[^{197}\text{Au}(^{139}\text{La},X)F_i]/\sigma[^{197}\text{Au}(p,X)F_i]$$

should have a constant value $\gamma^{\text{Au}}_{\text{La}}/\gamma^{\text{Au}}_p$ for any fragment F_i. We also make use of the hypothesis of limiting fragmentation which states that for sufficiently high projectile energies the cross section for production of the fragment F_i is independent of energy.

The concept of factorization has been tested for a

TABLE I. Cross sections for one-neutron removal reactions by ^{139}La projectiles on Co and Au targets.

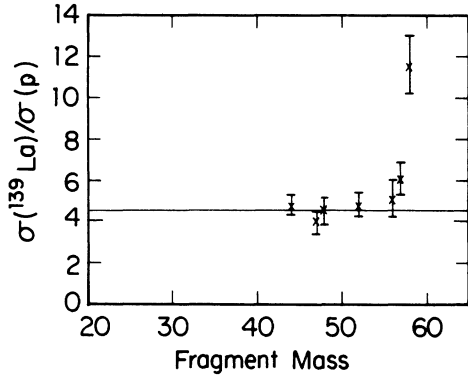| Reaction	Energy (GeV/nucleon)	Total beam intensity (particles)	Cross section (b)	% Correction secondary reactions
^{59}Co(^{139}La,X)^{58}Co	1.26	1.0×10^{10}	0.45±0.03	4
^{197}Au(^{139}La,X)^{196}Au	1.26	4.0×10^{10}	2.13±0.12	1

FIG. 2. The experimentally determined ratio $\sigma[^{59}\mathrm{Co}(^{139}\mathrm{La},X)F_i]/\sigma[^{59}\mathrm{Co}(p,X)F_i]$. The solid horizontal line indicates the weighted average for the above ratio using four points ranging from ^{44}Sc to ^{52}Mn.

variety of targets using a number of relativistic heavy ions. This includes low mass[16] Cu, intermediate mass,[17] Ag, and high mass[18] Au targets. Factorization was found to be approximately true. A more detailed discussion of these results as applied to estimation of ED cross sections is given in Ref. 4.

The concept of limiting fragmentation has been thoroughly studied for Au target fragmentation by Kaufman and co-workers.[18−20] They found that although the formation cross section for ^{196}Au by protons was essentially independent of energy above 200 MeV, limiting fragmentation applied[19,20] for deep spallation products only after the proton energy was higher than 10 GeV. The similarity in the shape of the $\sigma(\mathrm{RHI})/\sigma(p)$ curves for 4.8 and 25 GeV ^{12}C projectiles[18] gives one confidence that limiting fragmentation is approximately valid for 2.1 GeV/nucleon ^{12}C, at least in the range $60 < A < 190$. We thus assume limiting fragmentation to be a valid concept for the RHI used in this experiment.

We estimate the nuclear part of the one-neutron removal channel from ratios such as

$$\sigma[^{197}\mathrm{Au}(^{139}\mathrm{La},X)F_i]/\sigma[^{197}\mathrm{Au}(p,X)F_i]$$

as a function of the fragment mass. Since the limiting fragmentation region for protons is not reached for deep spallation products at least until 10 GeV, as discussed above, we used the proton cross sections measured by us at 28 GeV which are consistent with the measurements
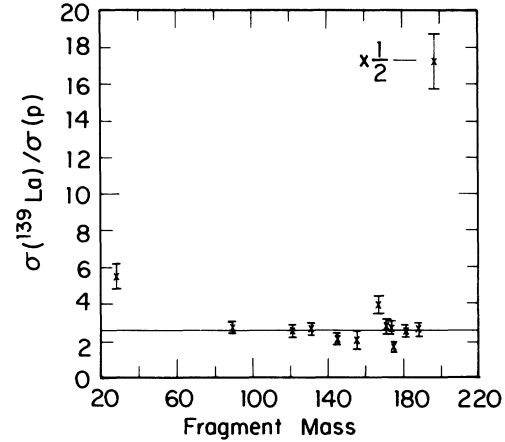

FIG. 3. The experimentally determined ratio $\sigma[^{197}\mathrm{Au}(^{139}\mathrm{La},X)F_i]/\sigma[^{197}\mathrm{Au}(p,X)F_i]$. The solid horizontal line indicates the weighted average for the above ratio using 11 points from ^{89}Zr to ^{188}Pt. The above ratio for ^{196}Au is about 34 and is thus shown at $\frac{1}{2}$ its actual size.

by Kaufman et al.[20] at 11.5 and 300 GeV. If we assume, for example, factorization for the nuclear part of the $^{197}\mathrm{Au}(^{139}\mathrm{La},X)^{196}\mathrm{Au}$ cross section, then

$$\sigma_{\mathrm{nucl}}(^{139}\mathrm{La},{}^{196}\mathrm{Au}) = \left[\frac{\sigma(^{139}\mathrm{La},F_i)}{\sigma(p,F_i)}\right]_{\mathrm{ave}} \sigma(p,{}^{196}\mathrm{Au}) \ .$$

C. Results for nuclear contribution to one-neutron removal cross sections

For the ^{59}Co targets the ratio

$$\sigma[^{59}\mathrm{Co}(^{139}\mathrm{La},X)F_i]/\sigma[^{59}\mathrm{Co}(p,X)F_i]$$

is plotted in Fig. 2. The ratios were determined for seven fragments in the mass range from ^{44}Sc to ^{58}Co. As can be seen from Fig. 2, factorization is valid in the mass range from $A = 44$ to 52. The fragments ^{57}Co and ^{58}Co are enhanced due to ED and we do not use ^{56}Co in the above average for the same reason. The average ratio was determined as a weighted average of four individual fragment ratios with A between 44 and 52. The average ratio along with an estimate of the "nuclear" cross section for production of ^{58}Co is given in Table II. The uncertainty of the average ratio includes both statistical factors, uncertainties due to the deviation of the data from strict

TABLE II. Nuclear cross sections for one-neutron out products from Co and Au targets.

Reaction	Number of ratios	Ratio mass range (A)	$\left[\dfrac{\sigma[T(^{139}\mathrm{La},X)F_i]}{\sigma[T(p,X)F_i]}\right]^{\mathrm{a}}$	Nuclear cross section section (b)
$^{59}\mathrm{Co}(^{139}\mathrm{La},X)F_i$	4	44−52	4.54±0.50	0.177±0.022
$^{197}\mathrm{Au}(^{139}\mathrm{La},X)F_i$	11	89−188	2.55±0.45	0.16±0.03

$^{\mathrm{a}}T$ refers to the target nucleus.

factorization, and uncertainties in the ^{11}C monitor cross sections.

For the ^{197}Au targets the ratio

$$\sigma[^{197}\text{Au}(^{139}\text{La},X)F_i]/\sigma[^{197}\text{Au}(p,X)F_i]$$

is plotted in Fig. 3. The ratios were determined for 13 fragments in the mass range from ^{24}Na to ^{196}Au. The figure shows that factorization is approximately valid between $A = 89$ and 188. The ^{24}Na is enhanced for RHI due to central collisions and the ^{196}Au ratio is strongly enhanced due to ED. (For the ^{59}Co targets it was not possible to obtain a cross section for ^{24}Na due to the low intensity of the ^{139}La beam.) The average ratio with an estimate of the "nuclear" cross section for production of ^{196}Au is given in Table II.

V. ELECTROMAGNETIC DISSOCIATION CROSS SECTIONS FOR ONE-NEUTRON REMOVAL PROCESSES

A. The calculated cross section

The Weizsäcker-Williams method for virtual photons[5] was used to calculate the electromagnetic-dissociation portion of the appropriate one-neutron removal cross sections using a modification of a computer code of Cook.[21] The procedure and its limitations have been discussed in Sec. II of this paper. The only adjustable parameter in the calculation is the minimum impact parameter b_{min}. Rather than letting it vary arbitrarily we have chosen it to be of the form

$$b_c = r_0[A_p^{1/3} + A_t^{1/3} - X(A_p^{-1/3} + A_t^{-1/3})]$$

suggested by Vary,[22] where the A's refer to the projectile and target, respectively. b_c can be visualized as a radius characterizing the range of the short-range nuclear force. Outside of this range, nuclear processes are assumed to be very unlikely, whereas for impact parameters less than b_c nuclear interactions are assumed to dominate. We thus used b_c as a lower limit for the ED process.

In the expression for b_c, the term $r_0(A_p^{1/3} + A_t^{1/3})$ can be thought of as a "touching radius" for the two nuclei. The term $X(A_p^{-1/3} + A_t^{-1/3})$ is a curvature correction. The constants r_0 and X were determined[22] to be 1.34 and 0.75 fm, respectively. The functional form of b_c is suggested from Glauber theory[23] and the values for r_0 and X were from fits[22] to nucleon-nucleus and nucleus-nucleus calculations[24] and densities from electron scattering data.[25] The constants r_0 and X were reevaluated using the recent compilation of DeVries, DeJager, and DeVries[26] of nuclear charge radii. For nuclei relevant to

this work the new charge radii differed from the old values by 0.05 fm or less in a random manner. Changes in r_0 of 0.1 fm or less cause changes in the calculated σ_{ED} that are 20 mb or less and thus small compared to the experimental σ_{ED} errors.

The photonuclear cross section ^{59}Co$(\gamma,n)^{58}$Co used for the ^{59}Co targets was that measured by Alvarez et al.[27] The photonuclear cross section ^{197}Au$(\gamma,n)^{196}$Au used for the ^{197}Au targets was that given by Veyssiere et al.[28] but multiplied by a factor of 0.93 to conform to recent remeasurements by Berman et al.[29] Thus the calculated σ_{ED}'s reported by us for ^{197}Au targets in earlier work[4,8] should be multiplied by 0.93.

B. Measured ED cross section

We define the "measured" ED cross section to be the one-neutron removal cross section measured in this experiment minus the empirically determined nuclear cross section for the one-neutron removal process described in Sec. IV. The results are given in Table III. The uncertainties for the measured ED cross sections include uncertainties from both the total and nuclear cross sections. The results presented in this work for ^{139}La projectiles are combined with the earlier results for ^{12}C through ^{56}Fe projectiles[4] in Fig. 4 (for ^{59}Co targets) and Fig. 5 (for ^{197}Au targets). The measured total cross section, empirically derived nuclear cross section, calculated ED cross section, and the measured ED cross section for one-neutron out processes in ^{59}Co and ^{197}Au are plotted as a function of projectile Z in Figs. 4 and 5. The calculated σ_{ED}'s have been generated using the factor of 0.93 suggested[29] for the ^{197}Au targets.

VI. DISCUSSION

We report here the observation of electromagnetic dissociation in target fragmentation of light (^{59}Co) and heavy (^{197}Au) nuclei by relativistic ^{139}La projectiles. The effect was observed for the reaction in which one neutron was removed from the target nucleus. The ED effect can be seen to increase both with the Z of the projectile and the Z of the target and becomes quite large (almost 2 barns) for the ^{197}Au$(^{139}$La,$X)^{196}$Au reaction. The one-neutron removal cross sections can be described by an empirically determined nuclear part which uses the concept of factorization plus an ED part which uses a virtual photon spectrum determined by the Weizsäcker-Williams method folded in with the appropriate measured photonuclear (γ,n) cross section. Good agreement is generally observed between the calculated and measured ED cross sections but the calculated value lies higher than

TABLE III. ED cross sections for one-neutron removal reactions by ^{139}La projectiles on Co and Au targets.

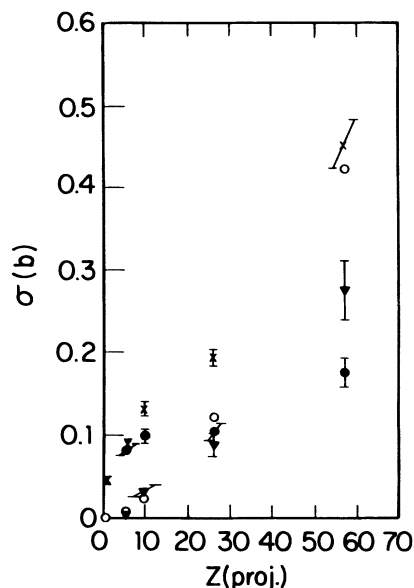| Reaction	Energy (GeV/nucleon)	Total σ (b)	Nuclear σ (b)	Measured σ_{ED} (b)	Calculated σ_{ED} (b)
^{59}Co$(^{139}$La,$X)^{58}$Co	1.26	0.45±0.03	0.177±0.022	0.28±0.04	0.43
^{197}Au$(^{139}$La,$X)^{196}$Au	1.26	2.13±0.12	0.16±0.03	1.97±0.13	2.34

FIG. 4. Various cross sections for the ^{59}Co(RHI,X)^{58}Co reaction as a function of projectile charge. The cross sections are measured total ($\times$), empirical nuclear ($\bullet$), calculated ED ($\circ$), and measured ED ($\blacktriangledown$).

the measured results for the heaviest (^{56}Fe and ^{139}La) projectiles.

In order to clarify the Z_p dependence of the ED cross sections, we present in Fig. 6 the measured and calculated σ_{ED} values on a log-log plot as a function of Z_p. If one assumes a simple power-law fit of the form $\sigma = \sigma_1 Z_p^b$, least-squares fits to the calculated ^{59}Co and ^{197}Au points give $b = 1.73$ and 1.80, respectively. Least-squares fits to
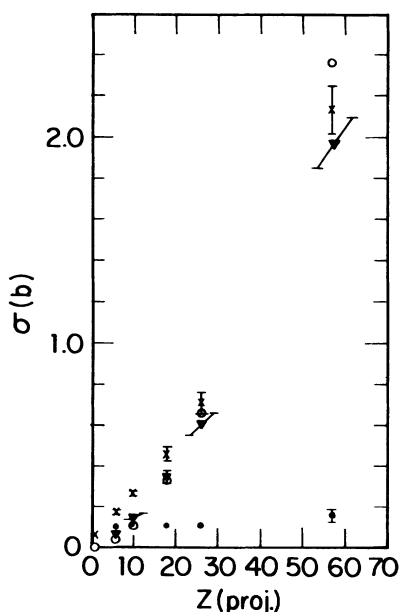
the experimental ^{59}Co and ^{197}Au points give $b = 1.48$ and 1.46, respectively. The standard deviations are 3.4 and 13.6 mb, respectively for the ^{59}Co and ^{197}Au experimental points indicating a surprisingly good fit to this empirical power-law form for σ_{ED}. For the ^{197}Au data, the fit to b of 1.46 is consistent with the fit obtained earlier[4] without the ^{139}La projectile data, adding strength to our earlier more speculative assertion that deviations from the WW calculations occur.

Calculations[4,6] using the WW method indicate that ED cross sections can become very large for high-Z projectiles at ultrarelativistic energies. It is now possible to test ED effects at Bevalac energies using ^{238}U projectiles. In Fig. 6 points representing the calculated one-neutron removal ED cross section for 0.96 GeV/nucleon ^{238}U projectiles on ^{59}Co and ^{197}Au targets are shown. These WW predictions are lower than our extrapolations from lower-mass projectiles due to the lower energy per nucleon available for ^{238}U. The calculation for a ^{197}Au target gives $4.8b$ whereas extrapolation of our empirical power-law fits would give a maximum of $3.8b$. Furthermore, one could anticipate an even lower value due to the lower energy per nucleon for ^{238}U.

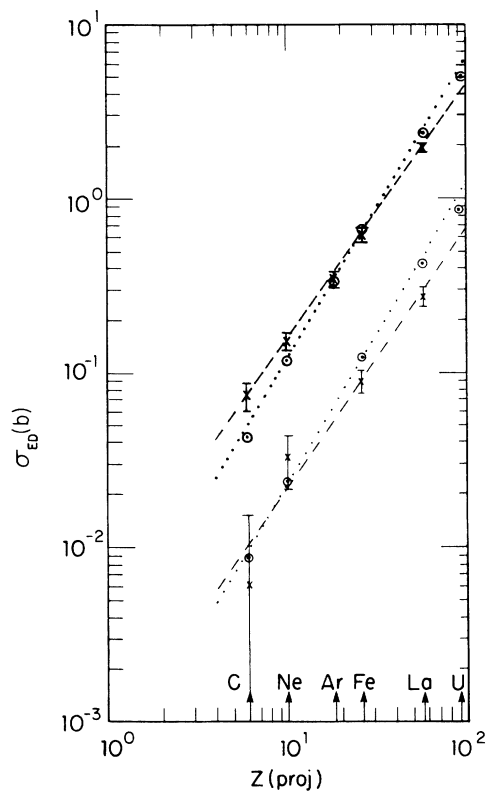This work implies that the ED cross section increases

FIG. 5. Various cross sections for the ^{197}Au(RHI,X)^{196}Au reaction as a function of projectile charge. The cross sections are measured total ($\times$), empirical nuclear ($\bullet$), calculated ED ($\circ$), and measured ED ($\blacktriangledown$). For some empirical nuclear cross sections the errors are less than the width of the circles.

FIG. 6. ED cross sections for the ^{197}Au(RHI,X)^{196}Au (upper curves) and ^{59}Co(RHI,X)^{58}Co (lower curves). The $\times$'s are measured points and circles are results of the WW calculation. The ^{139}La points are from this work and the other points are from previous work (Ref. 4). The empirical fits to both the calculated ($\odot$) and measured ($\times$) values are of the form $\sigma = \sigma_1 Z_p^b$ and are discussed in detail in the text.

with projectile charge less rapidly than predicted by the WW calculation. Reasonable adjustments of the parameters r_0 and X in the minimum impact parameter b_C change the magnitude of the ED cross sections but do not change significantly the slope of the curves in Fig. 6. A number of mechanisms can be considered in attempting to explain any deviations of the calculated ED cross sections from experiment for high-Z projectiles. Interference between Coulomb and nuclear processes would be expected to be small, since the nuclear effect is a small percentage of the total for high-Z projectiles. It is expected that interference between one and higher-order photon emission would also be small since it has been estimated[30] that high-order photon emission is less than 10% of the one photon emission process. Another possibility is the fact that the multipole mixture is different for real and virtual photons. This effect could be investigated by measuring ED cross sections at energies less than 1 GeV/nucleon since this should enhance the contribution of the lower-energy $E2$ giant resonance relative to the $E1$ resonance. It will be interesting to see if the deviations between theory and experiment implied in this work can be confirmed by experiments with relativistic ^{238}U beams.

At the energy of 100 GeV/nucleon planned for the RHIC collider, our WW calculation indicates that the ED cross section for the ^{197}Au(^{197}Au,X)^{196}Au reaction reaches 22b for stationary targets and 56b for colliding beams. These cross sections are much larger than the total hadronic cross section of about 6b. Such large total cross sections, if they exist, will impose constraints on the storage times for ultrarelativistic heavy ion beams[31,32] in colliders.

To summarize, we have extended measurements of ED cross sections for one-neutron removal from ^{59}Co and ^{197}Au targets in projectile Z up to ^{139}La projectiles. The WW calculations correctly predict the increase of the ED cross sections with both projectile and target Z, but appear to overestimate the cross section for high-Z projectiles. Large ED cross sections are predicted for the ultrarelativistic high-Z beams planned for future colliders but extrapolation of the presently available results to the above regime is risky. Measurements for the highest-Z projectiles at energies above 2 GeV/nucleon would be very illuminating.

ACKNOWLEDGMENTS

[1]H. H. Heckman and P. J. Lindstrom, Phys. Rev. Lett. **37**, 56 (1976).

[2]D. L. Olson, B. L. Berman, D. E. Greiner, H. H. Heckman, P. J. Lindstrom, G. D. Westfall, and H. J. Crawford, Phys. Rev. C **24**, 1529 (1981).

[3]M. T. Mercier, J. C. Hill, F. K. Wohn, and A. R. Smith, Phys. Rev. Lett. **52**, 898 (1984).

[4]M. T. Mercier, J. C. Hill, F. K. Wohn, C. M. McCullough, M. E. Nieland, J. A. Winger, C. B. Howard, S. Renwick, D. K. Matheis, and A. R. Smith, Phys. Rev. C **33**, 1655 (1986).

[5]J. D. Jackson, *Classical Electrodynamics*, 2nd ed. (Wiley, New York, 1975), p. 719.

[6]G. Baur and C. A. Bertulani, *Proceedings of the International School of Heavy Ion Physics, Erice, Italy, 1986*, edited by R. A. Broglia (Plenum, New York, 1987).

[7]J. C. Hill, F. K. Wohn, J. A. Winger, and A. R. Smith, Bull. Am. Phys. Soc. **32**, 1016 (1987).

[8]J. C. Hill, F. K. Wohn, J. A. Winger, and A. R. Smith, Phys. Rev. Lett. **60**, 999 (1988).

[9]R. Jäckle and H. Pilkuhn, Nucl. Phys. **A247**, 521 (1975).

[10]A. Goldberg, Nucl. Phys. **A240**, 636 (1984).

[11]C. A. Bertulani, Institut für Kernphysik, Kernforschungsanlage Jülich, Report ISSN 0343-7639, 1987.

[12]A. R. Smith, J. C. Hill, J. A. Winger, and P. J. Karol, Phys. Rev. C **38**, 210 (1988).

[13]L. K. Peker, Nucl. Data Sheets **42**, 457 (1984).

[14]J. Halperin, Nucl. Data Sheets **28**, 485 (1979).

[15]A. S. Goldhaber and H. H. Heckman, Ann. Rev. Nucl. Part. Sci. **28**, 161 (1978); R. M. Raisbeck and F. Yiou, Phys. Rev. Lett. **35**, 155 (1975); D. L. Olson, B. L. Berman, D. E. Greiner, H. H. Heckman, P. J. Lindstrom, and H. J. Crawford, Phys. Rev. C **28**, 1602 (1983).

[16]J. B. Cumming, R. W. Stoenner, and P. E. Haustein, Phys. Rev. C **14**, 1554 (1976); J. B. Cumming, P. E. Haustein, T. J. Ruth, and G. J. Virtes, *ibid.* **17**, 1632 (1978).

[17]N. T. Porile, G. D. Cole, and C. R. Rudy, Phys. Rev. C **19**, 2288 (1979).

[18]S. B. Kaufman, E. P. Steinberg, B. D. Wilkins, and D. J. Henderson, Phys. Rev. C **22**, 1897 (1980).

[19]S. B. Kaufman and E. P. Steinberg, Phys. Rev. C **22**, 167 (1980).

[20]S. B. Kaufman, M. W. Weisfield, E. P. Steinberg, B. D. Wilkins, and D. Henderson, Phys. Rev. C **14**, 1121 (1976).

[21]B. C. Cook (private communication).

[22]J. P. Vary (private communication).

[23]R. J. Glauber, in *High Energy Physics and Nuclear Structure*, edited by G. Alexander (North-Holland, Amsterdam, 1967), p. 311; W. Czys and L. C. Maximon, Ann. Phys. (N.Y.) **52**, 59 (1969).

[24]S. Barshay, C. B. Dover, and J. P. Vary, Phys. Rev. C **11**, 360 (1975).

[25]N. R. Collard, L. R. B. Elton, and R. Hofstader, in *Landolt-Börnstein: Numerical Data and Functional Relationships in Science and Technology*, edited by K.-H. Hellwege and H. Schopper (Springer, Berlin, 1967), Group I, Vol. 2, p. 21, and references therein.

[26]H. DeVries, C. W. DeJager, and C. DeVries, At. Data Nucl. Data Tables **36**, 495 (1987).

[27]R. A. Alvarez, B. L. Berman, D. D. Faul, F. H. Lewis, Jr., and P. Meyer, Phys. Rev. C **20**, 128 (1979).

[28]A. Veyssiere, M. Beil, R. Bergere, P. Carlos, J. Fagot, A. Lepretre, and A. de Miniac, Z. Phys. A **306**, 139 (1982).

[29]B. L. Berman, R. E. Pywell, S. S. Dietrich, M. N. Thompson, K. G. McNeill, and J. W. Jury, Phys. Rev. C **36**, 1286 (1987).

[30]G. Baur and C. A. Bertulani, Phys. Lett. B **174**, 23 (1986).

[31]G. R. Young, in *RHIC Workshop, Experiments for a Relativistic Heavy Ion Collider,* edited by P. E. Haustein and C. L. Woody, Brookhaven National Laboratory Report BNL-51921 (Brookhaven National Laboratory, New York, 1985), p. 27.

[32]R. M. DeVries and H. G. Fischer, in *Quark Matter Formation and Heavy Ion Collisions,* edited by M. Jacob and H. Satz (World-Scientific, Singapore, 1982), p. 513.